Pressure-induced softening of shear modes in wurtzite ZnO: A theoretical study

A. Zaoui[1,*] and W. Sekkal[1,2]
[1]*Max Planck Institut für Metallforschung, Heisenbergstrasse 3, D-70569 Stuttgart, Germany*
[2]*Staatliche Materialprüfungsanstalt (MPA), Universität Stuttgart, Pfaffenwaldring 32, 70569 Stuttgart, Germany*
(Received 22 February 2002; revised manuscript received 19 June 2002; published 12 November 2002)

Recent ultrasonic experiments on single-crystal specimens of the wurtzite ($B4$) phase of ZnO have shown that, under pressure, this material becomes softer against shear-type acoustic distortions. In the light of these results, we have performed atomistic calculations based on an interatomic pair potential within the shell-model approach. The focus is on the behavior of the elastic moduli C_{ij} as function of pressure. A linear evolution under pressure is observed for the two longitudinal modes C_{11} and C_{33} with a pressure derivative $\partial C/\partial P$ of 3.18 and 1.72, respectively. In contrast, the shear moduli C_{44} and C_{66} exhibit a negative pressure dependence throughout the pressure range with $\partial C_{44}/\partial P=-0.30$, and $\partial C_{66}/\partial P=-0.84$. We show that this behavior can be related to the wurtzite-rocksalt phase transition. Besides, the effect of phonons and the role of bond-bending forces as function of pressure in causing the elastic softening are discussed.

DOI: 10.1103/PhysRevB.66.174106 PACS number(s): 62.65.+k, 63.20.−e

I. INTRODUCTION

ZnO is a wide-band-gap semiconductor with a range of technological applications including electronic and electro-optic devices, catalysis, chemical sensors, and conductive solar cell window layers. If most of covalent II-VI compounds crystallize at normal conditions of temperature and pressure in a zinc blende or cinnabar structure, ZnO possesses an hexagonal wurtzite structure ($B4$). This phase transforms to the cubic rocksalt structure ($B1$) at a pressure in the vicinity of 9 GPa,[1,2] resulting in an increase of coordination number, from 4 to 6, and a large volume decrease of about 17%.[3] The zinc-blende phase ($B3$) is also known to exist,[4] but as a metastable state.

To date, several theoretical studies of both $B4$ and $B1$ phases using the linear combination of Gaussian-type orbitals Hartree-Fock (HF) method,[5] the full potential linear muffin-tin orbital approach to density-functional theory,[6] linearized augmented plane wave,[7] HF,[8] Gaussian type orbitals, local-density approximation (LDA), and generalized gradient approximation (GGA) methods[9] have been reported. However, these calculations were mostly limited to the $B4$, $B3$, and $B1$, and have not been applied to the eightfold coordinate of cubic $B2$ found at sufficiently high pressure.[9,10] Moreover, these studies have focused mainly to calculate the equilibrium transition pressure and not to explain the mechanism of the transition.

Recent ultrasonic experiments[11] on single-crystal specimens of the wurtzite phase of ZnO measure elastic moduli, from acoustic travel times. For the longitudinal moduli C_{11} and C_{33}, a linear dependence with positive values appears, while negative values are obtained for the shear moduli C_{44} and C_{66}. This unusual result has been found previously by Soga and Anderson[12] for the pressure derivative of the longitudinal sound velocity found to be positive, and the transverse one with a negative value. The goal of the present paper is motivated by the experimental measurements of Decremps, Zhang, and Li.[11] We will focus our study on pressure effect for the elastic behavior in ZnO using atomistic simulation techniques based on the shell model.[13] The latter has been found as a highly effective tool for prediction of different structural, and dynamical properties in ionic materials.[14–17] In Sec. II, we briefly describe the shell model potential parameters for ZnO. Results are summarized and discussed in Sec. III. Section IV contains the conclusion.

II. MODEL

In the present atomistic description, the lattice of a crystal is built from ions interacting via pair potentials and polarizable by means of the shell model.[13] The interatomic potential energy is then the sum of the long-range Coulombic and short-range non-Coulombic contributions. We use a simple analytical expression of the Buckingham type for the short-range interaction between ions i and j,

$$V_{ij}=A\exp(-r_{ij}/\varphi)-Cr_{ij}^{-6}, \tag{1}$$

where the term r^{-6} is referred to as the dispersive term. In the shell model,[13] each point ion consists of a core of charge X, and a shell of charge Y, such that the total charge is the sum of the core and shell charges. The potential parameters of the short-range pair potentials, A, φ, and C, as well as the shell model (Y) are obtained by empirical fitting to the properties of the wurtzite structure of ZnO.[18] These properties include the lattice constant, and elastic and dielectric constants.

Table I lists the model parameters representing the interatomic interactions in the lattice. The calculations were performed using the program GULP,[19] where the electrostatic interactions are evaluated both in real and in reciprocal space

TABLE I. Short-range potential and shell-model parameters for ZnO.

	A (eV)	φ (Å)	C (eV Å^6)	k (eV Å^{-9})
O_s-O_s^-	22 764.00	0.149	27.88	
Zn_c-O_s	700.30	0.338	0.0	
O_c-O_s				54.92

TABLE II. Calculated and experimental bulk properties for $B4$ (wurtzite), $B3$ (zinc blende), $B1$ (rocksalt), and $B2$ (CsCl) phases of ZnO.

Present work		LDA (Ref. 9)	GGA (Ref. 9)	Hartree-Fock (Ref. 5)	Experiment
$B4$					
V_0 (Å^3)	23.839	22.874	24.834	24.570	23.810,[a]23.790[b]
B_0 (GPa)	131.5	162.3	133.7	154.4	142.6,[a]183[b]
c/a	1.5663	1.6138	1.6076	1.5930	1.6021,[a]1.6018[b]
u	0.3895	0.3790	0.3802	0.3856	0.3823,[c]0.3819[d]
$B3$					
V_0 (Å^3)	23.848	22.914	24.854	24.551	
B_0 (GPa)	131.689	161.7	135.3	156.8	
$B1$					
V_0 (Å^3)	20.118	18.904	20.502	19.799	19.600,[a]19.484[b]
B_0 (GPa)	171.99	205.7	172.7	203.3	202.5,[a]228[b]
$B2$					
V_0 (Å^3)	18.551	18.073	19.785		
B_0 (GPa)	190.84	194.3	156.9		

[a]Value from Ref. 1.
[b]Value from Ref. 7.
[c]Value from Ref. 3.
[d]Value from Ref. 20.

according to the Ewald's method. The vibrational properties are calculated from the second derivatives of the energy by diagonalizing the dynamic matrix. The vibrational frequencies are the square root of the eigenvalues of the dynamical matrix. The elastic constants are calculated from a 6×6 matrix that contains the second derivatives of the energy density with respect to external strain.

III. RESULTS AND DISCUSSIONS

We present, first, the structural properties for the $B4$, $B3$, $B1$, and $B2$ phases of ZnO. All results given in Table II are obtained using N-P-T ensemble. This table contains results of previous first-principles calculations[5,9] as well as experimental data.[1,3,7,20] The wurtzite ZnO belongs to the $C_{6v}^4(P6_3mc)$ space group. The primitive cell includes two formula units, with all atoms occupying $2b$ sites of symmetry C_{3v}. The structure is described by two lattice constants, a and c, and the internal parameter u, whereas the zinc bende, rocksalt, and CsCl structures are described by one lattice constant (a). Conventional lattice constants are related to equilibrium volumes by $V_0=a^3/4$ $(B1,B3)$ and $a^3/2$ $(B2)$. For the $B4$ structure, $V_0=\sqrt{3}a^2c/4$. The obtained volume for the wurtzite and rocksalt structures is in excellent agreement with experiment (an accuracy of 0.1% for the wurtzite structure and of 2% for the rocksalt one). The bulk modulus for both structures is well described by our simulation. Our results agree also well with GGA calculations,[9] however, it is found that the LDA results[9] underestimate the equilibrium volume by about 4%, and overestimate the bulk modulus by 13%. The overall good agreement with experient and previous theoretical works indicates the reliability of the interatomic potential set and its transferability under high pressure. The calculation of the transition pressure from $B4$ to $B1$ and from $B1$ to $B2$ is deduced from the variation of the enthalpy versus pressure for both transitions. The wurtzite phase has the lowest enthalpy under low pressure while the rocksalt phase has the lowest enthalpy beyond the transition pressure; the zinc-blende phase is metastable. Our results for transitions pressures, volumes, and volume changes are given in Table III along with experimental[1,7] and previous theoretical data[9] for the $B4$ to $B1$ transition. We have found that the $B4$-$B1$ transition occurs at 10.45 GPa. This is in good agreement with the experimental value of 9.1 GPa,[1] and with GGA calculations (9.32 GPa), rather than LDA ones (6.6 GPa).[9] We notice also that there is a volume reduction across the $B4$ to $B1$ transition of about 15% in good agreement with the experimental value[1] of 17%. At a much higher pressure, we predict a transition from $B1$ to $B2$ near 352 GPa accompanied by a volume reduction of about 7%; the LDA and GGA transition pressure value is about 260 GPa and the volume reduction is around 5%.[9]

In order to check the reliability of the potential model, we have also calculated the static dielectric constant, the high-frequency dielectric constant, and the phonon modes for the wurtzite structure of ZnO. We found a static dielectric constant equal to 9.02, which is in good agreement with the value of 8.75 obtained by Hill and Waghmare using first-principle calculations.[21] The obtained high-frequency dielectric constant is equal to 2.3, while the experimental value is 3.95.[22]

Figure 1 displays the dispersion curve for the Γ-A direction. At the Γ point, it is predicted from group theory the existence of the following optic modes: A_1, E_1, two E_2, and two B_1 modes. The A_1, E_1, and E_2 modes are Raman active. In addition, A_1 and E_1 are infrared active, and therefore split into longitudinal and transverse optical (LO and TO) components. The B_2 modes are silent. The obtained values

TABLE III. Transition pressure values for $B4 \rightarrow B1$ ($T1$), and $B1 \rightarrow B2$ ($T2$) transitions in ZnO.

	Present work	LDA (Ref. 9)	GGA (Ref. 9)	Hartree-Fock (Ref. 5)	Experiment
P_{T1} (GPa)	10.45	6.60	9.32	8.57	9.1,[a] 8.7[b]
$V_{B4}(P_{T1})$ (Å^3)	22.215	22.029	23.346	23.358	22.481,[a] 22.783[b]
$V_{B1}(P_{T1})$ (Å^3)	19.041	18.341	19.515	19.037	18.799,[a] 18.804[b]
ΔV_1 (Å^3)	3.170	3.688	3.831	4.321	3.682,[a] 3.979[b]
P_{T2} (GPa)	352	260	256		
$V_{B1}(P_{T2})$ (Å^3)	10.507	11.977	12.340		
$V_{B2}(P_{T2})$ (Å^3)	10.084	11.377	11.738		
ΔV_2 (Å^3)	0.420	0.600	0.602		

[a]Value from Ref. 1.
[b]Value from Ref. 7.

for wurtzite-ZnO are listed in Table IV and are compared to experimental data.[23,24]. The corresponding curve is qualitatively and quantitatively in reasonable agreement with previous works.[23,24]

Let us focus on the behavior of the elastic properties of the wurtzite structure of ZnO under pressure up to the phase-transition pressure to the rocksalt phase. In Table V, the obtained elastic values for C_{11}, C_{33}, C_{44}, and C_{66} at zero pressure are listed and are compared to the experimental measurements.[25] The agreement found is, in general, good. In Figs. 2 and 3, we display the variation of C_{11}, C_{33}, C_{44}, and C_{66} as function of pressure. A linear behavior appears for all variations. However, a positive slope is noticed in the case of Fig. 2, while the slope is negative in Fig. 3. The pressure derivative for the two longitudinal modes C_{11} and C_{33} is equal to 3.186 and 1.722, respectively. By contrast, the shear moduli C_{44} and C_{66} exhibit a negative pressure dependence with $\partial C_{44}/\partial P = -0.30$, and $\partial C_{66}/\partial P = -0.84$. This behavior has been observed recently by Decremps, Zhang, and Li,[11] where the elastic moduli were calculated from ultrasonic wave velocity measurements. In addition, they found that this phenomenon is also observed at higher temperatures, and that the pressure derivatives of the elastic shear modes become more negative.

These unusual negative values for both shear modes could

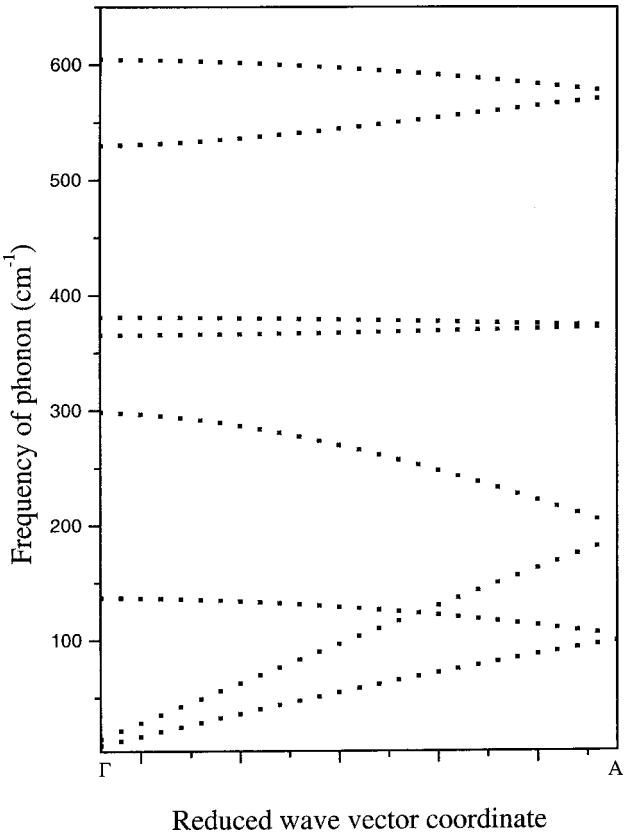

FIG. 1. Dispersion curve of $B4$ phase for the Γ-A direction.

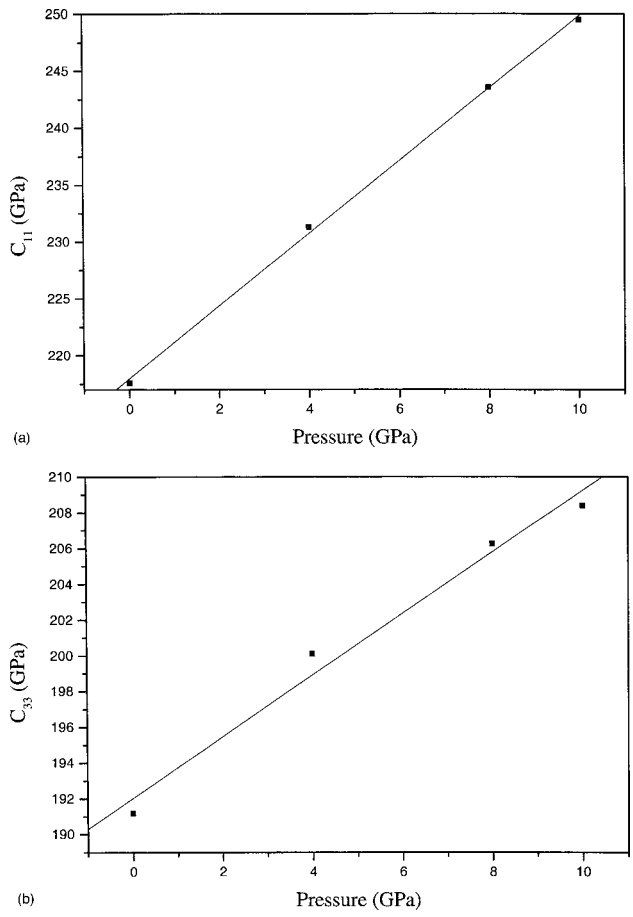

FIG. 2. Elastic constants versus pressure. (a) C_{11}, (b) C_{33}.

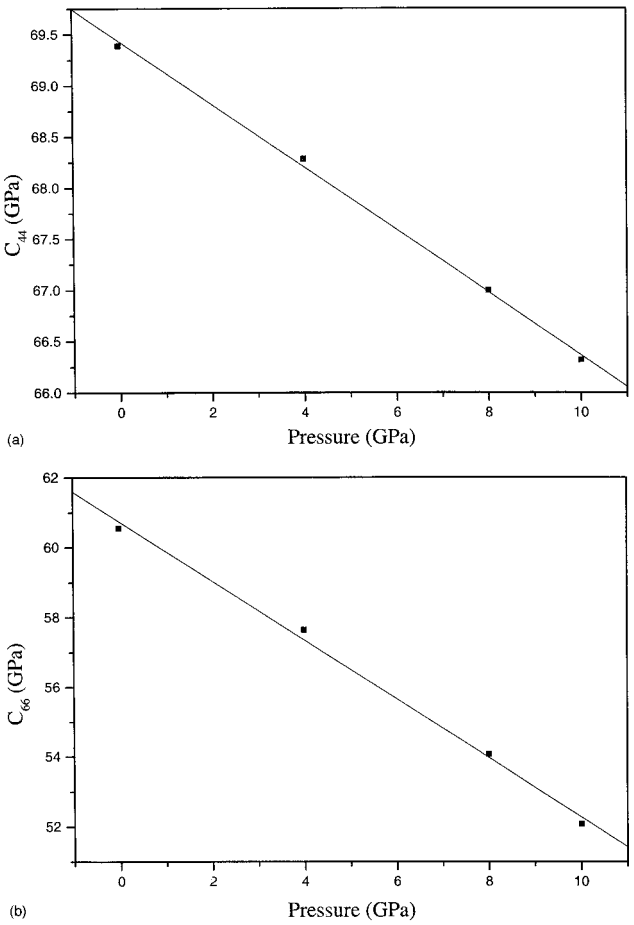

FIG. 3. Elastic constants versus pressure. (a) C_{44}, (b) C_{66}.

be related to the simultaneous effect of a major contribution of the second-nearest-neighbor interactions to the transverse acoustic phonon modes. Another possibility to explain the observed shear softening is to involve the pressure evolution of bond-bending forces.[11] According to the work of Zaoui *et al.*,[26] we have calculated the bond-bending quantity (β) from the following equation.[26]

$$\beta = \frac{2d}{\sqrt{3}} \frac{C_{11} - C_{12}}{2},$$

TABLE IV. Phonon frequencies of zone center in the wurtzite ZnO.

Phonon mode	Frequency (cm^{-1}) (present work)	Frequency (cm^{-1}) (experiments)
E_2	126	101,[a] 98[b]
A_1-TO	382	380,[a] 392[b]
E_1-TO	316	413,[a] 436[b]
E_2	335	444,[a] 465[b]
A_1-LO	548	579,[a] 570[b]
E_1-LO	628	591,[a] 585[b]

[a]Value taken from Ref. 23.
[b]Value taken from Ref. 24.

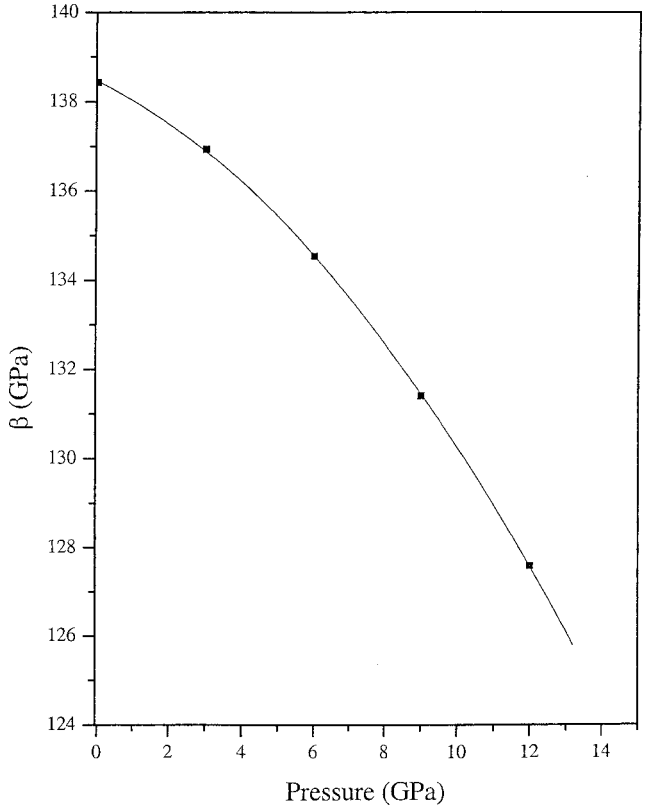

FIG. 4. The bond-bending forces versus pressure.

where d is the nearest-neighbor distance.

In Fig. 4, we plot the variation of β as a function of pressure P. It appears that the bond bending β decreases under pressure relating to the following equation:

$$\beta = 138.4545 - 0.39371P - 0.04286P^2.$$

This quantity is directly linked to the elastic constants and the ionicity of the bond. This is discussed in a previous paper.[26] In other previous works, we have correlated the variation of the ionicity to high-pressure structural phase transition.[27] We think that the ionicity decreases under pressure since the charges become less delocalized favoring a more strong covalency of the bond up to a certain critical value where the initial atomic arrangement becomes less appropriate. This forces the system to transform to another structure with different atomic arrangement. In general, the first preference is the structure with higher coordination number.

Even if the chemical bonding (i.e., ionicity) is not illustrated from our atomistic calculations, the related quantities,

TABLE V. Elastic constant for ZnO in the wurtzite structure.

	C_{11} (GPa)	C_{13} (GPa)	C_{33} (GPa)	C_{44} (GPa)	C_{66} (GPa)
Present work	231	104	183	72	60
Experiment (Ref. 25)	207–209	101–106	209–221	44.1–46.1	44.5–44.6

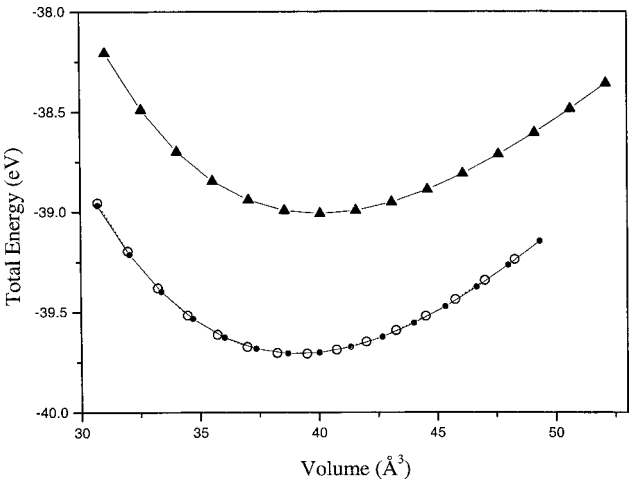

FIG. 5. Total energies versus volume for the two states of tetragonal phase: unrelaxed (triangle) and relaxed (empty circle). The rocksalt structure is represented by filled circles.

i.e., bond bending forces, confirm our assumptions and show a decreasing behavior under pressure. Therefore, our finding for the elastic softening matches the expected variation found experimentally.

Obviously, the weakening of C_{44} and C_{66} tends to destabilize the wurtzite structure leading to a structural change due to a microscopic shearing on certain crystallographic planes. In order to see what kind of structural changes the soft C_{44} and C_{66} imply, we calculate the pressures at which C_{44} and C_{66} vanish. We found that they remain high at the $B4$-$B1$ transition pressure (10.45 GPa), and vanish at a pressure beyond the transition, around 50 GPa. The corresponding structure is found to be a metastable tetragonal phase with $a=b=2.459$ Å and $c=3.478$ Å. However, after relaxing this structure at various pressures, we found that the relaxed structure has an energetic curve (Fig. 5) similar qualitatively and quantitatively to that found for the rocksalt structure, with a minimum total energy $E=-39.705$ eV, for a volume $V_{\min}=20.14$ Å^3. The energetic difference between the two structures corresponds to 0.005 eV, while the difference between their bulk modulus is 3.79 GPa. From Fig. 5 we have also extracted the energetic difference between the two states of tetragonal structure (unrelaxed and relaxed), which gives a weak value of 0.696 eV.

This implies that the soft elastic behavior should result in the structural transformation from the $B4$ to $B1$ phase. We may conclude that the elastic softening behavior gives a higher transition pressure (50 GPa) than the thermodynamics prediction of 10.45 GPa. This phenomenon appears also in the case of MgO,[28] for which the authors studied the elastic instability.

This behavior could also be related to the effect of phonons in the wurtzite-NaCl transition. In order to clarify this relationship, we have calculated the elastic moduli with and without optimization of atomic positions. Our results show a change for the obtained values of the elastic constants with an important increase in the case of C_{44} (13%), and a weak change in the case of C_{66} (3%).

Additionally, in a more recent work, Decremps *et al.*[22] studied the high-pressure behavior of optical phonons in $B4$ phase of ZnO using room-temperature Raman spectroscopy and *ab initio* calculations based on a plane-wave pseudopotential method within the density-functional theory. They found that the LO-TO splitting of the E_1 phonon mode is weakly pressure dependent, and the E_2^{low} is the only mode that exhibits a negative pressure dependence. All other modes increase with pressure, and no anomaly up to the transition pressure is detected. Therefore, no softening of the optic A_1 and E_2^{high} modes is shown, as expected theoretically.[29]

VI. CONCLUSION

Atomistic simulations of the wurtzite phase of ZnO were presented using the shell-model potentials in order to investigate the behavior of longitudinal (C_{11} and C_{12}) and shear (C_{44} and C_{66}) modes under pressure. The obtained results confirm the previous experimental works in which ZnO becomes softer against shear-type acoustic distortions. The pressure derivative of C_{11} and C_{33} is equal to 3.18 and 1.72, respectively, while it corresponds to -0.30 and -0.84 for C_{44}, and C_{66}, respectively. Our calculations show that the soft elastic behavior can be related to the wurtzite-rocksalt transition. The effect of phonons and the role of bond-bending forces with pressure in causing the elastic softening was also discussed. Besides, the transition pressures from the $B4$ to $B1$, and from $B1$ to $B2$ structures, as well as the dielectric constant and the phonon modes of the $B4$ phase have been discussed.

ACKNOWLEDGMENT

We wish to thank the Max-Planck-Institute für Metallforschung for financial support during the realization of the present work.

*Electronic address: zaoui@marvin.mpi-stuttgart.mpg.de

[1] S. Desgreniers, Phys. Rev. B **58**, 14 102 (1998).
[2] J. M. Recio, M. A. Blanco, V. Luana, R. Pandey, L. Gerward, and J. S. Olsen, Phys. Rev. B **58**, 8949 (1998).
[3] C. H. Bates, W. B. White, and R. Roy, Science **137**, 993 (1962).
[4] W. H. Bragg and J. A. Darbyshire, J. Met. **6**, 238 (1954).
[5] J. E. Jaffe and A. C. Hess, Phys. Rev. B **48**, 7903 (1993).
[6] R. Ahuja, L. Fast, O. Eriksson, J. M. Wills, and B. Johansson, J. Appl. Phys. **83**, 8065 (1998).
[7] H. Karzel, W. Potzel, M. Kofferlein, W. Schiessl, M. Steiner, U. Hiller, G. M. Kalvius, D. W. Mitschell, T. P. Das, P. Blaha, K. Schwartz, and M. P. Pasternack, Phys. Rev. B **53**, 11 425 (1996).
[8] M. Recio, P. Pandey, and V. Luana, Phys. Rev. B **47**, 3401 (1993).
[9] J. A. Jaffe, J. A. Snyder, Z. Lin, and A. C. Hess, Phys. Rev. B **62**, 1660 (2000).
[10] L. Gunn Liu and W. A. Bassett, *High-Pressure Phases With Implications for the Earth's Interior* (Oxford Univeristy, New York, 1986).
[11] F. Decremps, J. Zhang, and B. Li, Phys. Rev. B **63**, 224105 (2001).

[12] N. Soga and O. L. Anderson, J. Appl. Phys. **38**, 2985 (1967).
[13] B. G. Dick and A. W. Overhauser, Phys. Rev. **112**, 90 (1958).
[14] M. R. Aouas, W. Sekkal, and A. Zaoui, Solid State Commun. **120**, 413 (2001).
[15] P. Zapol, R. Pandey, and J. Gale, J. Phys.: Condens. Matter **9**, 9517 (1997).
[16] P. Zapol, R. Pandey, M. Ohmer, and J. Gale, J. Appl. Phys. **79**, 671 (1996).
[17] R. Pandey, M. C. Ohmer, and J. Gale, J. Phys.: Condens. Matter **10**, 5525 (1998).
[18] G. V. Lewis and C. R. A. Catlow, J. Phys. C **18**, 1149 (1985).
[19] J. D. Gale, J. Chem. Soc., Faraday Trans. **93**, 629 (1997).
[20] J. Albertsson, S. C. Abrahams, and A. Kvick, Acta Crystallogr., Sect. B: Struct. Sci. **B45**, 34 (1989).
[21] N. A. Hill and U. Waghmare, Phys. Rev. B **62**, 8802 (2000).
[22] F. Decremps, J. Pellicer-Porres, A. M. Saitta, J.-C. Cheervin, and A. Polian, Phys. Rev. B **65**, 092101 (2002).
[23] C. A. Arguello, D. L. Rousseau, and S. P. S. Porto, Phys. Rev. **181**, 1351 (1969).
[24] M. Rajalakshmi, A. K. Arora, B. S. Bendre, and S. Mahamuni, J. Appl. Phys. **87**, 2445 (2000).
[25] G. Carlotti, D. Einstte, G. Sonian, and D. Vamma, J. Phys. Condens. Matter **7**, 9147 (1995).
[26] A. Zaoui, M. Ferhat, M. Certier, H. Aourag, and B. Khelifa, Phys. Lett. A **228**, 378 (1997).
[27] A. Zaoui, M. Certier, M. Ferhat, and B. Khelifa, Solid State Commun. **99**, 659 (1996).
[28] B. B. Karki, G. J. Ackland, and J. Crain, J. Phys.: Condens. Matter **9**, 8579 (1997).
[29] S. Limpijumnong and W. R. L. Lambrecht, Phys. Rev. Lett. **86**, 91 (2001); J. Serrano, A. Rubio, E. Hernández, A Muñoz, and A. Mujica, Phys. Rev. B **62**, 16 612 (2000).